

Analog RoF Fronthaul Carrying 27.6-Tb/s CPRI-equivalent Rate and 512-QAM with Sideband Modulation for IQ Imbalance Separation and Bi-directional Transmission

Yixiao Zhu^{1,3,*}, Xiansong Fang^{2,3}, Chenbo Zhang², Yicheng Xu¹, Qunbi Zhuge¹, Xiaopeng Xie², Weisheng Hu¹, Fan Zhang^{2,*}

¹State Key Laboratory of Advanced Optical Communication System and Networks, Shanghai Jiao Tong University, Shanghai, 200240, China

²State Key Laboratory of Advanced Optical Communication System and Networks, Peking University, Beijing, 100871, China

³These authors contributed equally to this work

*Corresponding authors: yixiaozhu@sjtu.edu.cn, fzhang@pku.edu.cn

Abstract: We leverage sideband modulation-based bidirectional scheme to separate the transmitter-side IQ imbalance and boost the SNR to 30.8dB. We experimentally demonstrate high-capacity coherent analog RoF fronthaul achieving 27.6Tb/s(=12λ×2.089Tb/s) CPRI-equivalent rate and 512-QAM over 10-km SSMF. © 2024 The Author(s)

1. Introduction

There is an urgent demand for capacity upgrades in cloud radio access networks (C-RAN) due to both the increasing number of end users and the bandwidth-intensity services. Fronthaul bridges mobile and optical communications by delivering wireless signals through optical fibers between the centralized /distributed unit (CU/DU) and radio units (RUs) [1]. As the wireless signal bandwidth is significantly boosted from 20-MHz in 4G to 100/400-MHz in 5G and even higher in the future, the common public radio interface (CPRI) becomes incapable [2]. Advanced radio-over-fiber (RoF) techniques are expected to satisfy the requirement of capacity and fidelity [3]. Following the trend of dense small cells, the classic analog RoF is revived due to its high spectral efficiency and simple structure [4].

The main challenge of analog RoF lies in the signal-to-noise ceiling of ~25 dB, which hinders the transmission of high-order modulation format wireless signals [3]. For coherent detection systems, the limitation can be attributed to two aspects: 1) the frequency-dependent IQ imbalance-induced image band crosstalk; 2) the time-varying laser phase noise-induced constellation rotation. For the IQ crosstalk issue, transmitter-side calibration [5] or post-equalization [6] schemes have been proposed. Using a ‘Golden’ coherent receiver, optical spectrum analyzer, or direct detection receiver as a reference, the transmitter-side IQ imbalance can be measured and compensated. Meanwhile, receiver-side real-valued 4×4 multi-input-multi-output (MIMO) equalizers are also applicable for mitigation. Alternatively, based on single-sideband (SSB) modulation and heterodyne coherent detection, both transmitter- and receiver-side IQ image bands are mapped to outside the signal spectrum, leading to record 10-GBd dual-polarization (DP) probabilistic-shaped 16384-ary quadrature amplitude modulation (PS-16384-QAM) transmission [7]. For the laser phase noise issue, a straightforward way is employing Hz-level ultra-narrow-linewidth lasers to suppress the penalty from reduced angles between neighboring constellation points [8], which are unaffordable in cost-sensitive scenarios. Besides, digital phase-locked loop (PLL)-integrated equalizers are capable of phase tracking [9]. However, the time-domain pilot symbol-aided mode is not compatible with the transmission requirement of analog RoF, and the decision-directed mode is not stable due to the decision error, especially for high-order formats.

In this work, we adopt sideband modulation to separate the IQ crosstalk and improve the signal-to-noise ratio (SNR) to >30 dB, and IQ modulator bias-induced residual optical carrier for redundancy-free phase tracking in analog RoF fronthaul. The left and right sidebands (LSB/RSB) are utilized for bi-directional transmission, where the crosstalk is further suppressed by the reflection ratio. After 10-km standard single-mode fiber (SSMF), 12λ×17-GHz wavelength-division-multiplexed (WDM) DP 512-QAM signals can achieve the 15.3% open forward error correction (O-FEC) threshold of 1.8×10⁻² with 100-kHz laser sources. The sum linewidth and symbol duration product is 1.18×10⁻⁵. The single-channel CPRI-equivalent rate is 2.09Tb/s within only 18.85-GHz optical bandwidth.

2. Sideband modulation-based IQ imbalance separation and residual carrier-based phase tracking

The impact of IQ imbalance is illustrated in Fig. 1, which results from the imperfect splitting ratio, amplitude mismatch α , and $\pi/2$ phase deviation $\Delta\theta$. Assuming the in-phase and quadrature components of the original signal s to be I and Q , the generated signal s' can be represented and decomposed as

$$s' = I + \alpha e^{j(\pi/2+\Delta\theta)} Q = (s + s^*)/2 + \alpha e^{j(\pi/2+\Delta\theta)} (s - s^*)/2 = (1 + \alpha e^{j\Delta\theta}) s/2 + (1 - \alpha e^{j\Delta\theta}) s^*/2 \quad (1)$$

We can find that the IQ imbalance would introduce conjugated image crosstalk overlapped with the original signal, which would be frequency-dependent if the S21 response of arbitrary waveform generator (AWG), electrical

amplifier (EA), and IQ modulator is considered [7]. Fortunately, by up-converting the original signal for LSB or RSB modulation, the image band moves to the opposite frequency region and can be separated. For amplifier-less short-reach scenarios, the noise only comes from the transceiver, and the in-band SNR is thus significantly improved. To fully utilize the other sideband, bi-directional transmission can be implemented, where the IQ crosstalk from the opposite sideband would be further attenuated by the reflection ratio of the fiber link.

Additionally, a residual optical carrier is used for format-transparent and redundancy-free carrier recovery [10]. As shown in Fig. 1(b), we manually bias the IQ modulator above the null point for residual optical carrier generation. In the receiver-side DSP, we first search the peak of the signal spectrum, and down-convert it to the baseband for frequency offset estimation (FOE). We then extract the residual carrier using a narrow-bandwidth low-pass filter. The phase noise is removed by conjugation and multiplication. Note that compared to the digital pilot tone, residual optical carrier does not sacrifice the AWG effective number of bits (ENoB), and is not affected by the IQ imbalance.

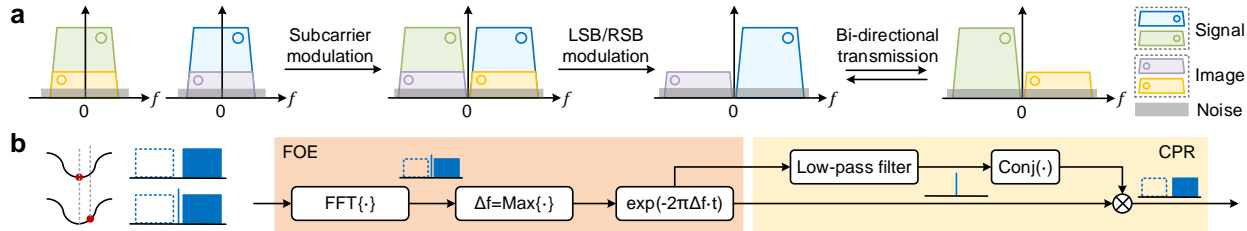


Fig. 1. (a) Signal spectra with baseband, subcarrier, and sideband modulations in the presence of IQ crosstalk. LSB/RSB: left/right sideband. (b) IQ modulator bias-based carrier recovery. FOE: frequency offset estimation; CPR: carrier phase recovery.

3. Experimental setup and DSP

The experimental setup of 12-channel WDM coherent analog RoF fronthaul is shown in Fig. 2(a). At the transmitter, we use a 1550-nm external cavity laser (ECL) with 100-kHz linewidth as an optical source of the channel under test (CUT). The 17-Gbaud LSB/RSB 512-QAM signal is generated by a 120-GSa/s AWG (Keysight M8194), amplified by a pair of 50-GHz electrical amplifiers (EA, SHF), and then modulated through a 27-GHz 3-dB bandwidth IQ modulator (EOspace). The bias is deviated from the null point to introduce a residual carrier with ~ 15 dB carrier-to-signal power ratio. For the loading channels, 11 ECLs spacing at 50 GHz are combined and fed into IQ modulator 2 simultaneously. The CUT and loading channels are respectively amplified, polarization division multiplexed, and combined using a wave-shaper (Finisar). After 10-km SSMF transmission, an optical band-pass filter (OBPF) is placed to select the desired wavelength. The demultiplexed signal is intradyne coherent detected with a 100-kHz local oscillator (LO). After four 70-GHz BPDs detection and 50-GHz EAs amplification, the electrical waveform is captured by a 128-GSa/s real-time oscilloscope (RTO, Keysight UXR0594AP) for offline DSP. In the transmitter-side DSP, 32768 512-QAM symbols are mapped from binary bits, which is framed by a 3072-symbol preamble for synchronization and channel equalization. After up-sampling, root-raised cosine shaping is conducted with a roll-off of 0.1. Then the sequence is digitally up-converted for LSB and RSB modulation, in which a 1-GHz guard band is

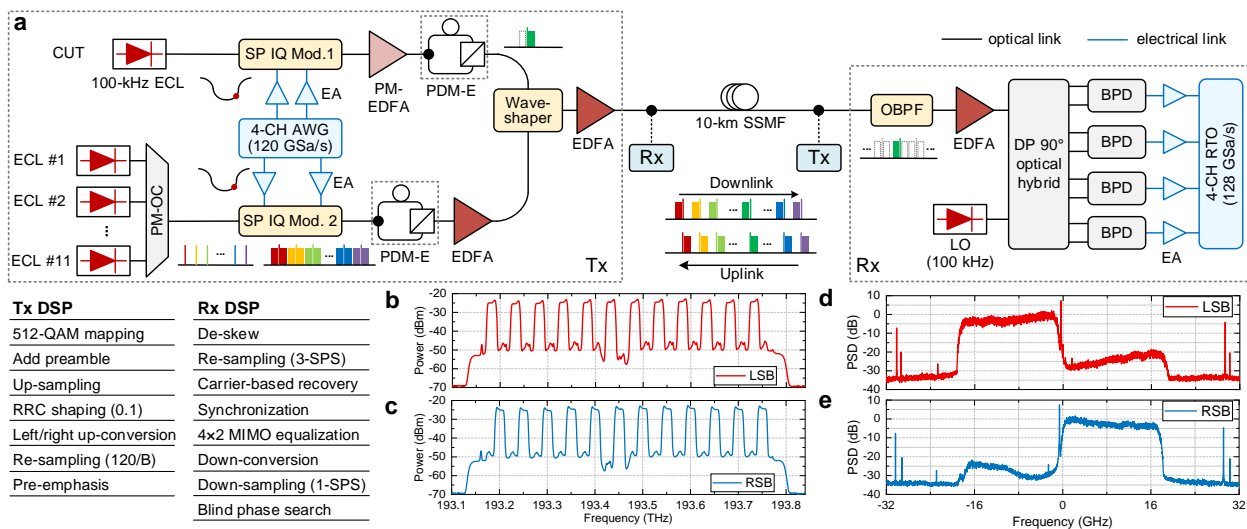


Fig. 2. (a) Experimental setup and DSP stacks. CUT: channel under test; ECL: external cavity laser; SP IQ Mod.: single-polarization IQ modulator; AWG: arbitrary waveform generator; PM-EDFA: polarization-maintaining erbium-doped fiber amplifier; PDM-E: polarization-division-multiplexing emulator; EA: electrical amplifier; OC: optical coupler; SSMF: standard single-mode fiber; OBPF: optical band-pass filter; BPD: balanced photodiode; RTO: real-time oscilloscope. Measured optical spectra of 12-channel WDM signals with (b) LSB and (c) RSB modulation. Measured electrical spectra with (d) LSB and (e) RSB modulation. RRC: root-raised cosine; SPS: sample-per-symbol.

reserved for residual carrier. After re-sampling to AWG sampling rate, linear pre-emphasis is applied to improve the bandwidth response. In the receiver-side DSP, the detected waveform is 3-time re-sampled, frequency and phase recovered by the residual carrier, synchronized and equalized based on the preamble. The MIMO equalizer has 3-order sparse Volterra kernels with lengths of (81, 11, 11). We use the blind phase search algorithm to finely correct the residual phase noise within $\pm 8^\circ$. The measured optical spectra of the 12-channel WDM signals with LSB and RSB modulation are shown in Fig. 2(b) and 2(c). The received electrical spectra of LSB and RSB are also displayed in Fig. 2(d) and 2(e). The residual carrier behaves like a pilot tone around zero frequency. The IQ imbalance-induced crosstalk is ~ 20 dB lower than the signal. The tones around ± 30 GHz come from the AWG clock.

4. Experimental results and discussion

We first optimize the SNR dependence on the symbol rate at back-to-back (BTB) in Fig. 3(a). The SNR can achieve 30.8 dB at 17-GBd, which can satisfy the 29.1-dB SNR (equivalent to 3.5% EVM) requirement of 256-QAM format. The SNR gradually degrades with symbol rate, which is attributed to the increased in-band noise and bandwidth limitation. The LSB and RSB exhibit consistent SNR for similar performance during bi-directional transmission. We then evaluated the bit-error rate (BER) versus modulation formats of 128/256/512-QAM at 17-GBd in Fig. 3(b). The recovered constellations are provided for an intuitive understanding of the signal quality. All the constellation points are distinguishable. Fig. 3(c) shows the measured BER versus receiver optical power (ROP) at BTB. The sensitivity is approximately -18 dBm at the 15.3% O-FEC threshold. The power budget is not only benefited from the optical amplifier in the signal branch, but also the beating gain with the clean LO. We further evaluate 12-channel WDM transmission over 10-km SSMF in Fig.3(d). The BER values of all channels in both downlink and uplink are well below the O-FEC threshold [26]. From the performance of phase noise compensation, we achieve sum linewidth and symbol duration product of 1.18×10^{-5} as shown in Fig. 3(e). Moreover, we compare the conversion efficiency from aggregated wireless bandwidth to optical bandwidth in single channel. Traditional IFoF scheme has the advantages of low cost but halved efficiency due to intensity modulation. PM, DPCM, DSM, and DA-RoF schemes all benefited from the SNR gain of bandwidth expansion. In comparison, analog RoF with sideband modulation and coherent detection achieves 2-Tb/s/ λ CPRI-equivalent rate with 512-QAM using only 18.85-GHz optical bandwidth.

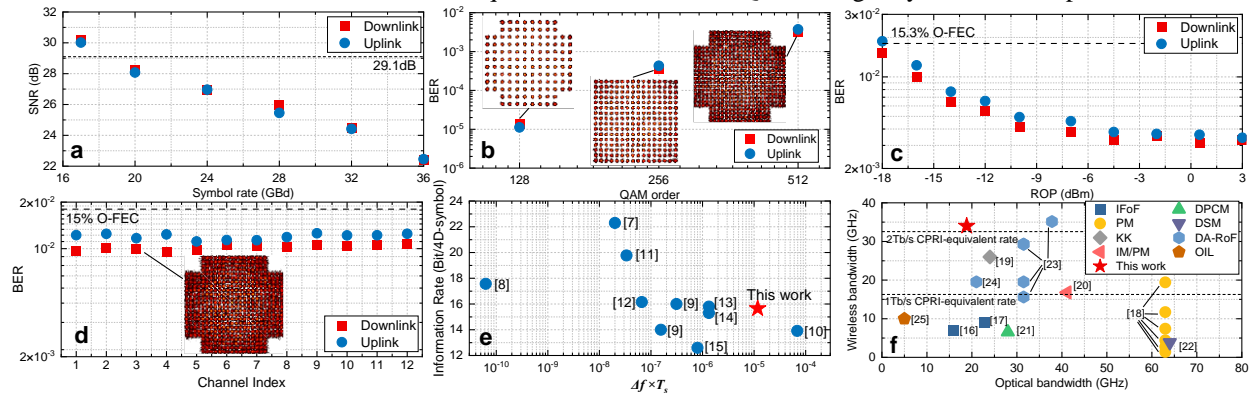


Fig. 3. (a) Measured SNR versus symbol rate with 512-QAM at BTB. (b) Measured BER versus modulation formats at BTB. (c) Measured BER versus ROP with 512-QAM at BTB. (d) Measured BER versus channel index with 12- λ WDM DP 512-QAM signals at 10-km SSMF. (e) Information rate versus sum linewidth and symbol duration product. (f) Aggregated wireless bandwidth versus optical bandwidth in single channel. IFoF: intermediate-frequency-over-fiber; PM: phase modulation; KK: Kramers-Kronig receiver; DPCM: differential pulse coded modulation; DSM: delta-sigma modulation; DA-RoF: digital-analog RoF; OIL: optical injection-locking.

4. Conclusions

In summary, we leverage sideband modulation to improve the SNR to >30 dB by suppressing the IQ crosstalk, and employ residual optical carrier for redundancy-free phase tracking in analog RoF fronthaul. 27.6Tb/s ($=12\lambda \times 2.089$ Tb/s) CPRI-equivalent rate and 512-QAM signals transmission over 10-km SSMF is experimentally demonstrated. The results show the potential of analog RoF for spectrally-efficient and high-fidelity fronthaul.

Acknowledgments National Key R&D Program of China (2022YFB2903500), and NSFC (62271305, 62001287).

References

- [1] A. Pizzinat, et al., JLT, **33**(5), 1077 (2015).
- [2] CPRI Specification V7.0, Oct. 2015.
- [3] D. Che, et al., JLT, **39**(16), 5325 (2021).
- [4] X. Liu et al., JLT, **34**(6), 1556 (2022).
- [5] X. Chen, et al., Proc. OFC'2021, Th5D.3.
- [6] T. Kobayashi, et al., Proc. OFC'2019, Th4B.2.
- [7] X. Chen, et al., Proc. ECOC'2019, 1-4.
- [8] M. Nakamura, et al., Proc. ECOC'2022, We3C.5
- [9] M. Nakamura, et al., Proc. OFC'2022, M3H.1.
- [10] X. Fang, et al., Proc. ECOC'2023, Th.C.1.8.
- [11] S. L. I. Olsson, et al., OE, **26**(4), 4522 (2018).
- [12] X. Chen, et al., OE, **27**(21), 29916 (2019).
- [13] M. Terayama, et al., Proc. OFC'2018, Th1F.2.
- [14] S. Beppu, et al., OE, **23**(4), 4960 (2015).
- [15] Y. Wang, et al., OE, **26**(13), 17015 (2018).
- [16] K. Tanaka, et al., Proc. OFC'2022, W4C.2.
- [17] K. Tanaka, et al., Proc. ECOC'2022, We1F.2.
- [18] D. Che, et al., Proc. ECOC'2020, Th3B-1.
- [19] S. T. Le, et al., Proc. ECOC'2018, We4B.4.
- [20] S. Ishimura, et al., JLT, **36**(8), 1478 (2018).
- [21] L. Zhang, et al., IEEE Comm. Mag. **57**(4), 131 (2019).
- [22] J. Wang, et al., JLT, **36**(2), 568 (2018).
- [23] Y. Zhu, et al., Proc. ECOC'2022, Th3A.5.
- [24] Y. Zhu, et al., Proc. OFC'2023, Th4C.6.
- [25] M. Yoshida, et al., JLT, **39**(5), 1289 (2021).
- [26] W. Wang, et al., JLT, **41**(3), 926 (2023).